



相对论密度泛函理论研究晕核的近期进展

张开元 潘琮 陈思宇 罗庆金 吴柯岩 向一峰

Recent Progress on Halo Nuclei in Relativistic Density Functional Theory

ZHANG Kaiyuan, PAN Cong, CHEN Siyu, LUO Qingjin, WU Keyan, XIANG Yifeng

在线阅读 View online: <https://doi.org/10.11804/NuclPhysRev.41.2023CNPC28>

引用格式:

张开元, 潘琮, 陈思宇, 罗庆金, 吴柯岩, 向一峰. 相对论密度泛函理论研究晕核的近期进展[J]. 原子核物理评论, 2024, 41(1):191–199. doi: 10.11804/NuclPhysRev.41.2023CNPC28

ZHANG Kaiyuan, PAN Cong, CHEN Siyu, LUO Qingjin, WU Keyan, XIANG Yifeng. Recent Progress on Halo Nuclei in Relativistic Density Functional Theory[J]. Nuclear Physics Review, 2024, 41(1):191–199. doi: 10.11804/NuclPhysRev.41.2023CNPC28

您可能感兴趣的其他文章

Articles you may be interested in

基于相对论Hartree–Fock理论的原子核壳结构性质研究

Nuclear Shell Structure Properties Described by Relativistic Hartree–Fock Theory

原子核物理评论. 2020, 37(3): 478–491 <https://doi.org/10.11804/NuclPhysRev.37.2019CNPC61>

能量密度泛函中不同对关联处理方式对原子核形变描述影响的探讨

Effect of Different Pairing Correlations on the Description of Nuclear Deformations within Energy Density Functional Framework

原子核物理评论. 2020, 37(1): 26–33 <https://doi.org/10.11804/NuclPhysRev.37.2020006>

相对论离子与氦二聚体碰撞电离的理论研究

Theoretical Study on the Ionization Process of Relativistic Ion and Helium Dimer Collisions

原子核物理评论. 2022, 39(3): 391–395 <https://doi.org/10.11804/NuclPhysRev.39.2022041>

复动量表象方法对奇特核中晕现象的研究

Study on Halo Phenomenon in Exotic Nuclei by Complex Momentum Representation Method

原子核物理评论. 2020, 37(3): 574–579 <https://doi.org/10.11804/NuclPhysRev.37.2019CNPC07>

相对论平均场研究超子星

Investigation on the Hyperonic Star in Relativistic Mean–field Model

原子核物理评论. 2022, 39(2): 135–153 <https://doi.org/10.11804/NuclPhysRev.39.2022013>

理想磁流体力学中的相对论性Kelvin圈积分定理

Relativistic Kelvin Circulation Theorem for Ideal Magnetohydrodynamics

原子核物理评论. 2020, 37(3): 679–683 <https://doi.org/10.11804/NuclPhysRev.37.2019CNPC19>

Article ID: 1007-4627(2024)01-0191-09

Recent Progress on Halo Nuclei in Relativistic Density Functional Theory

ZHANG Kaiyuan¹, PAN Cong^{2,†}, CHEN Siyu¹, LUO Qingjin¹, WU Keyan¹, XIANG Yifeng¹

(1. Institute of Nuclear Physics and Chemistry, China Academy of Engineering Physics, Mianyang 621900, Sichuan, China;
2. Department of Physics, Anhui Normal University, Wuhu 241000, Anhui, China)

Abstract: Since the discovery of the halo nucleus ^{11}Li in 1985, halo phenomena in exotic nuclei have always been an important frontier in nuclear physics research. The relativistic density functional theory has achieved great success in the study of halo nuclei, e.g., the self-consistent description of halo nucleus ^{11}Li and the microscopic prediction of deformed halo nuclei. This paper introduces some recent progresses based on the deformed relativistic Hartree-Bogoliubov theory in continuum (DRHBc) and the triaxial relativistic Hartree-Bogoliubov theory in continuum (TRHBc). A microscopic and self-consistent description of the deformed halo nucleus ^{37}Mg , including its small one-neutron separation energy, large root-mean-square radius, diffuse density distribution, and p -wave components for the halo neutron, has been achieved by the DRHBc theory. The DRHBc theory has also predicted a deformed neutron halo and the collapse of the $N=28$ shell closure in the recently discovered isotope ^{39}Na . The TRHBc theory has been newly developed and applied to the aluminum isotopic chain. The heaviest odd-odd ^{42}Al has been predicted as a triaxial halo nucleus with a novel shape decoupling between its core and halo at the triaxial level.

Key words: halo phenomena; relativistic density functional theory; ^{37}Mg ; ^{39}Na ; ^{42}Al

CLC number: O571.21 **Document code:** A **DOI:** [10.11804/NuclPhysRev.41.2023CNPC28](https://doi.org/10.11804/NuclPhysRev.41.2023CNPC28)

0 Introduction

The discovery of the first halo nucleus^[1] in 1985 has attracted great interest. The radius of a halo nucleus significantly deviates from the empirical formula $r_0A^{1/3}$ (where $r_0 \approx 1.2$ fm and A is the mass number), shaking the simple assumption that the nucleus is incompressible. Therefore, the description of halo phenomena has challenged traditional models for nuclear structure. The experimental exploration of halo nuclei also has been stimulating the development of new generations of radioactive ion beam facilities worldwide.

During the past decades, about 20 halo nuclei or candidates have been identified or suggested in experiments, as shown in Fig. 1. On the theoretical side, the nuclear models studying halo phenomena include the few-body model^[2–3], shell model^[4–5], antisymmetrized molecular dynamics^[6–7], halo effective field theory^[8–9], nonrelativistic^[10–11] and relativistic density functional theories^[12–13], etc.

The relativistic density functional theory is designed for nuclear many-body problems based on the quantum

field theory and density functional theory^[15]. Due to many appealing advantages^[16–17], such as the automatic inclusion of the spin-orbital coupling^[18–19] and the reasonable description of its isospin dependence^[20], the competition between scalar and vector densities giving rise to the new saturation mechanism^[21], natural explanation of the pseudospin symmetry in the nucleon spectrum^[22–24] and the spin symmetry in antinucleon spectrum^[24–26], and self-consistent treatment of the nuclear magnetism^[27–28], the relativistic density functional theory has become one of the most popular nuclear theories^[15, 29–38].

In the study of halo nuclei, great progress has been achieved based on the relativistic density functional theory. The relativistic continuum Hartree-Bogoliubov (RCHB) theory^[12, 39], which solves the relativistic Hartree-Bogoliubov (RHB) equation in coordinate space by assuming the spherical symmetry, is suitable for describing spherical exotic nuclei. Based on the RCHB theory, the halo phenomenon in ^{11}Li was described in a microscopic and self-consistent way^[12], the giant halo formed by more than two neutrons was predicted^[40], and the neutron halo in hypernuclei was explored^[41].

Received date: 30 Jun. 2023; Revised date: 21 Jan. 2024

Foundation item: National Natural Science Foundation of China (12305125, U2230207, U2030209); Natural Science Foundation of Sichuan Province (124NSFSC5910); National Key R&D Program of China (2020YFA0406001, 2020YFA0406002)

Biography: ZHANG Kaiyuan (1995–), male, Tongchuan, Shaanxi Province, Ph.D., working on nuclear physics; E-mail: zhangky@caep.cn

† Corresponding author: PAN Cong, E-mail: cpan@ahnu.edu.cn

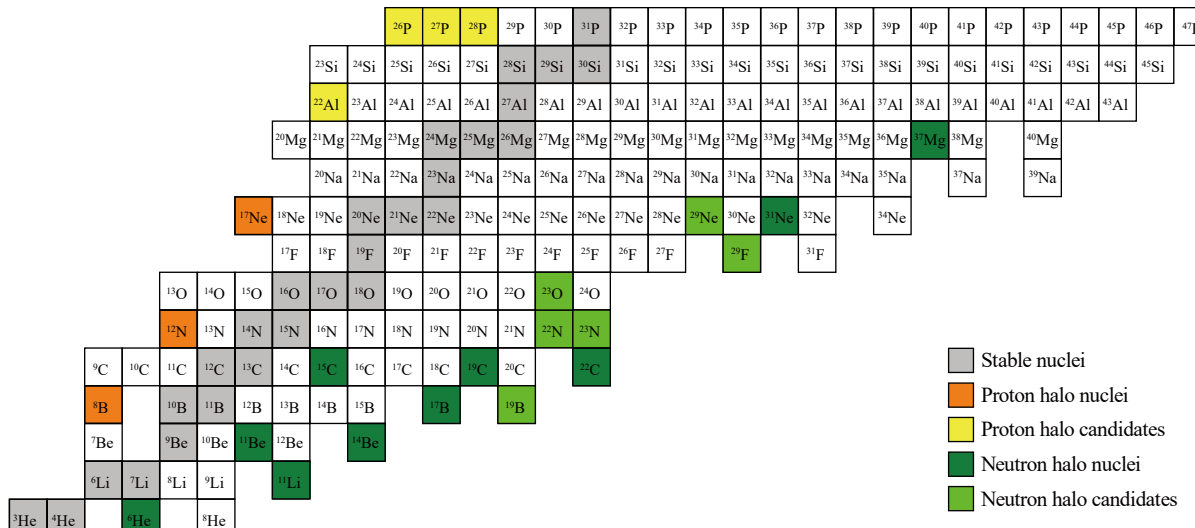


Fig. 1 Experimentally known nuclear landscape from helium to phosphorus, where stable nuclei and experimentally confirmed/suggested neutron as well as proton halo nuclei/candidates are indicated by grey, olive/green, and orange/yellow colors, respectively. Taken from Ref. [14] and slightly modified. (color online)

The deformed relativistic Hartree-Bogoliubov theory in continuum (DRHBC)^[42–45], which considers the axial deformation and solves the RHB equation in a Dirac Woods-Saxon (DWS) basis^[46], can provide an adequate description for axially deformed exotic nuclei. The DRHBC theory has predicted the deformed halo nuclei $^{42,44}\text{Mg}$ and the shape decoupling between the core and the halo^[42–43], which is considered one of the interesting new phenomena near the drip line^[47]. While the heaviest magnesium isotope synthesized in the laboratory so far is ^{40}Mg ^[48] and the DRHBC prediction for $^{42,44}\text{Mg}$ remains to be verified, many known halo nuclei have been successfully described using the DRHBC theory, including $^{17,19}\text{B}$ ^[49–50], $^{15,19,22}\text{C}$ ^[51–52], ^{31}Ne ^[53], and ^{37}Mg ^[54–55]. A deformed two-neutron halo in ^{39}Na has also been predicted by the DRHBC theory^[14]. In addition, a DRHBC mass table including both deformation and continuum effects is under construction^[56–59]. During this construction, many interesting phenomena have been investigated or predicted using the DRHBC theory^[60–69]. The DRHBC theory has also been extended with the angular momentum projection, enabling the exploration of rotational excitations of deformed halo nuclei^[70–71].

It should also be mentioned that there are many studies on deformed halos using other models, *e.g.*, the single-particle model^[72], antisymmetrized molecular dynamics^[73], Hartree-Fock theory^[74–75], Hartree-Fock-Bogoliubov theory^[76–77], relativistic Hartree-Fock-Bogoliubov theory^[78–79], and *ab initio* theory^[80]. Most of these studies have assumed axial symmetry for nuclear deformation.

The triaxial relativistic Hartree-Bogoliubov theory in continuum (TRHBC)^[81], which considers the triaxial deformation and solves the RHB equation in the DWS basis,

has been developed very recently in order to explore triaxially deformed halo nuclei. The observed heaviest odd-odd aluminum isotope, ^{42}Al ^[48], has been predicted as a triaxial halo nucleus with a novel shape decoupling between the core and the halo at the triaxial level^[81].

This paper is structured as follows. The frameworks of the DRHBC and TRHBC theories are briefly presented in Section 1. Several of the above mentioned studies on halo nuclei are introduced in Section 2, including ^{37}Mg , ^{39}Na , and ^{42}Al . A summary is given in Section 3.

1 The DRHBC and TRHBC theories

In the following we briefly introduce the main formalism for the DRHBC and TRHBC theories. Starting from a meson-exchange or point-coupling Lagrangian density, the RHB equation,

$$\begin{pmatrix} h_D - \lambda & \Delta \\ -\Delta^* & -h_D^* + \lambda \end{pmatrix} \begin{pmatrix} U_k \\ V_k \end{pmatrix} = E_k \begin{pmatrix} U_k \\ V_k \end{pmatrix}, \quad (1)$$

can be derived by treating the nuclear mean field and pairing correlations on the same footing^[82]. In Eq. (1), λ is the Fermi energy, and E_k and $(U_k, V_k)^T$ are respectively the quasiparticle energy and the quasiparticle wave function. h_D denotes the Dirac Hamiltonian,

$$h_D(\mathbf{r}) = \alpha \cdot \mathbf{p} + V(\mathbf{r}) + \beta[M + S(\mathbf{r})], \quad (2)$$

with the scalar potential $S(\mathbf{r})$ and the vector potential $V(\mathbf{r})$. Δ represents the pairing potential,

$$\Delta(\mathbf{r}_1, \mathbf{r}_2) = V^{\text{pp}}(\mathbf{r}_1, \mathbf{r}_2) \kappa(\mathbf{r}_1, \mathbf{r}_2), \quad (3)$$

where V^{pp} is the pairing interaction and κ is the pairing tensor. The present DRHBC and TRHBC theories adopt a density-dependent zero-range pairing interaction,

$$V^{pp}(\mathbf{r}_1, \mathbf{r}_2) = V_0 \frac{1}{2} (1 - P^\sigma) \delta(\mathbf{r}_1 - \mathbf{r}_2) \left[1 - \frac{\rho(\mathbf{r}_1)}{\rho_{sat}} \right], \quad (4)$$

in which V_0 is the pairing strength, $(1 - P^\sigma)/2$ is the projection operator for the spin-zero component, and ρ_{sat} is the saturation density of nuclear matter.

In the DRHBC theory for axially deformed nuclei, the densities and potentials are expanded as follows,

$$f(\mathbf{r}) = \sum_l f_l(r) P_l(\cos \theta), \quad (5)$$

where P_l is the l -order Legendre polynomial, and the assumed spatial reflection symmetry limits l to being even numbers.

In the TRHBC theory for triaxially deformed nuclei, the densities and potentials are expanded in terms of spherical harmonics,

$$f(\mathbf{r}) = \sum_{lm} f_{lm}(r) Y_{lm}(\theta, \varphi). \quad (6)$$

The spatial reflection symmetry and the mirror symmetries with respect to xy , xz , and yz planes lead to the limitations that l and m are even numbers and $f_{lm}(r) = f_{l-m}(r)$ ^[83].

The RHB equations are solved in the DWS basis^[46, 84], whose wave function has a more appropriate asymptotic behavior compared with the harmonic oscillator basis and is thus suitable for expanding the wave functions of weakly bound nuclei.

In practical calculations, an energy cutoff of $E_{cut} = 300$ MeV and an angular momentum cutoff of $J_{max} = 23/2 \hbar$ for the DWS basis can guarantee the convergence of numerical results^[56]. In such a basis space, the pairing strength $V_0 = -325$ MeV·fm³, the saturation density $\rho_{sat} = 0.152$ fm⁻³, and a pairing window of 100 MeV can reproduce the odd-even mass differences of calcium and lead isotopes^[56]. For light nuclei, it is enough to truncate the Legendre or spherical harmonic expansion at $l_{max} = 6$ ^[85]. The blocking effects in odd-mass and odd-odd nuclei are taken into account via the equal filling approximation^[44, 58, 86].

2 Recent progress

2.1 The halo nucleus ^{37}Mg

The deformed p -wave neutron halo nucleus ^{37}Mg , confirmed experimentally in 2014^[87–88], is the heaviest nuclear halo system to date. Although ^{37}Mg had been synthesized and identified in 1996^[89], theoretical studies over the subsequent two decades, including phenomenological calculations based on a Woods-Saxon potential^[90] and microscopic ones based on nonrelativistic and relativistic density functional theories^[91–93], did not predict its neutron halo. Even after 2014, a fully microscopic description

of the neutron halo in ^{37}Mg remained a challenge. For instance, a large quadrupole deformation ($\beta_2 \gtrsim 0.5$) must be introduced in the calculations based on Woods-Saxon potentials so as to reproduce the p -wave occupation of the valence neutron in ^{37}Mg ^[94–97]. The calculations based on the antisymmetrized molecular dynamics reproduced the matter radii of $^{24–36}\text{Mg}$ but significantly underestimated the matter radius of ^{37}Mg ^[73, 98]. The results from nonrelativistic Hartree-Fock-Bogoliubov calculations were found to be density-functional dependent^[76–77, 99], with only the M3Y-P6 functional capable of providing the p -wave components of the valence neutron in ^{37}Mg ^[76].

The deformed p -wave neutron halo in ^{37}Mg has been described in a microscopic and self-consistent way using the DRHBC theory^[54]. Fig. 2 illustrates the two-dimensional neutron density distributions for $^{35–37}\text{Mg}$ in the DRHBC calculations with the density functional PC-F1^[100]. The neutron density distribution of ^{37}Mg is remarkably more diffuse, which is consistent with the picture of nuclear halos. The root-mean-square (rms) radii for $^{35–37}\text{Mg}$ calculated from nuclear densities are respectively 3.44, 3.49, and 3.57 fm, in satisfactory agreement with the empirical radii of 3.44(03), 3.49(01), and 3.62(03) fm deduced from the reaction cross sections^[73]. Furthermore, the densities and the wave function of the valence neutron from the DRHBC theory can be fed as microscopic inputs into the Glauber model to study reaction observables, which turns out successful in describing the halo nucleus ^{31}Ne ^[53]. Such a work for magnesium isotopes has also been performed recently, and the reaction cross section of ^{37}Mg bombarding a carbon target and the longitudinal momentum distribution of ^{36}Mg fragments after its breakup are reproduced very well^[55].

To further understand the halo phenomenon in ^{37}Mg , Fig. 3 presents the single-neutron orbitals around the Fermi energy and their rms radii. It is found that the rms radius of the weakly bound orbital 5 is approximately 5.6 fm, significantly larger than others. Orbital 5 is occupied by the valence neutron in ^{37}Mg , with 38% $2p_{1/2}$ and 19% $2p_{3/2}$ components, which are comparable to the $\approx 40\%$ p -wave halo components suggested in experiments^[87]. The low centrifugal barrier for p waves allows considerable tunneling of the wave function into the classically forbidden region, which, together with the weak binding of orbital 5, results in its largest rms radius. While certain s - and p -wave components are found for orbitals 1 and 2, respectively, the diffuseness of their wave functions is suppressed by the relatively deep binding. For orbitals 3 and 4 dominated respectively by d and f waves and orbitals 6 and 7 with the occupation probabilities $\lesssim 0.1$, their contribution to the neutron halo in ^{37}Mg is marginal. Therefore, it is natural to decouple the neutron density of ^{37}Mg into a core and a halo, with the Fermi energy as a threshold. As seen in Fig. 2, the core density closely resembles that of ^{36}Mg ,

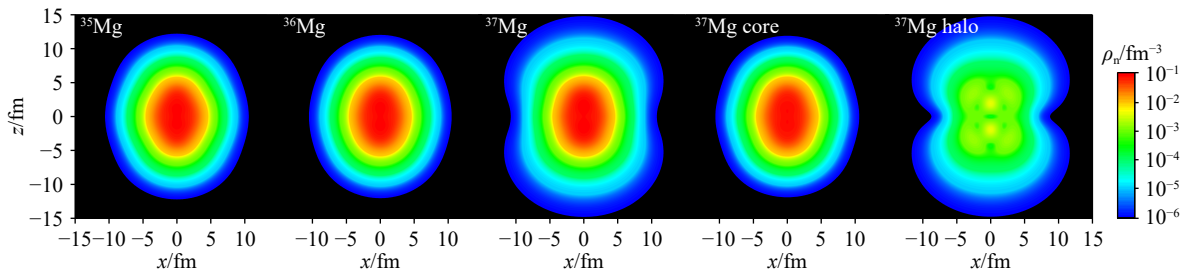


Fig. 2 Two-dimensional neutron density distributions for $^{35-37}\text{Mg}$ as well as ^{37}Mg 's core and halo in the xz plane with z being the symmetry axis. Taken from Ref. [54]. (color online)

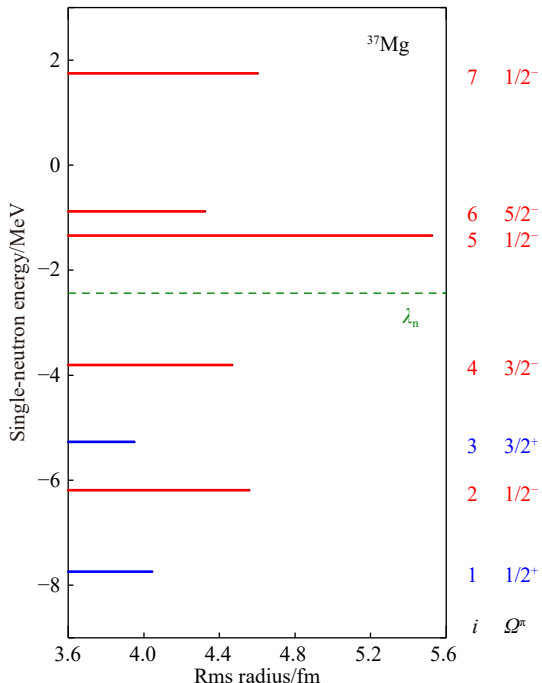


Fig. 3 Energy versus rms radius for single-neutron orbitals around the Fermi energy λ_n (dashed line) in the canonical basis for ^{37}Mg . The order i and quantum numbers Q^π are given on the right. Taken from Ref. [54].

while the halo density predominantly contributes to the total neutron density far away from the center.

The results from DRHBC calculations based on other density functionals, such as PC-PK1^[101], NL3^{*}^[102], and PK1^[103], are quantitatively consistent with the above results. Therefore, the microscopic self-consistent description of the DRHBC theory on the halo nucleus ^{37}Mg is essentially density-functional independent. It is regrettable that the DRHBC theory was only applied to the even-even nuclei in magnesium isotopes before 2014, missing the prediction of the neutron halo in ^{37}Mg .

2.2 The new isotope ^{39}Na

The exploration of the boundaries in nuclear chart, *i.e.*, drip-line locations, has always been a major goal of nuclear physics^[104]. Although the proton drip line has been experimentally delineated up to neptunium with $Z=93$ ^[105], the neutron drip line is only known up to neon with $Z=$

10^[106]. In 2022, further experimental exploration discovered the currently most neutron-rich isotope of sodium with $Z=11$, ^{39}Na , but the neutron drip line has not been determined yet^[107]. The neutron number of ^{39}Na is $N=28$, a traditional magic number. The disappearance of traditional magic numbers and the emergence of new ones are novel phenomena in exotic nuclei near drip lines, *e.g.*, the disappearance of the $N=28$ magicity in the isotones of ^{39}Na , ^{40}Mg and ^{42}Si ^[108-109]. On the other hand, as shown in Fig. 1, clues to halo nuclei or candidates are found in every isotopic chain from He to P, except for Na and Si. Therefore, it is necessary to study the shell structure of ^{39}Na and explore possible halo phenomena in neutron-rich Na isotopes, which could provide references for future experiments.

Figure 4 shows the evolution of single-neutron levels around the Fermi energy with the quadrupole deformation obtained from DRHBC calculations with PC-PK1. In the spherical limit, the orbitals $2p_{3/2}$ and $1f_{7/2}$ are nearly degenerate and close to the $2p_{1/2}$. In the traditional shell model, there is a sizable energy gap between $1f_{7/2}$ and $2p_{3/2}$, forming the $N=28$ shell closure and making the spherical shape energetically favored. In ^{39}Na , the lowering of $2p$ orbitals results in the collapse of the $N=28$ shell closure, and the down-sloping levels split from the $1f_{7/2}$ orbital leads to a large ground-state deformation of $\beta_2 > 0.4$.

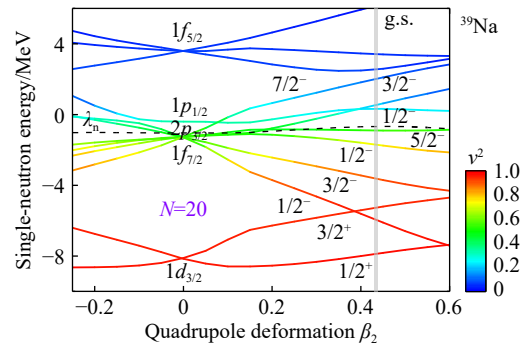


Fig. 4 Single-neutron levels around the Fermi energy λ_n (dashed line) of ^{39}Na in the canonical basis from constrained calculations. Their quantum numbers $n\ell j$ in the spherical limit and Q^π on the prolate side are labeled. The occupation probability v^2 is scaled by colors. The grey vertical line corresponds to the ground state (g.s.) of ^{39}Na . Taken from Ref. [14]. (color online)

In addition, as shown in Fig. 4, the pairing correlations lead to the partial occupation of the weakly bound or continuum $1/2^-$ and $3/2^-$ orbitals by the valence neutrons in ^{39}Na . Due to the deformation effect, the pf components are mixed in the wave functions of these orbitals, and the p -wave components in valence neutrons favor the formation of a neutron halo. Therefore, the halo phenomenon may exist in ^{39}Na .

Figure 5 shows the neutron density distributions along and perpendicular to the symmetry axis for the odd-mass Na isotopes with $N \geq 20$. The ground-state deformation of ^{31}Na is spherical due to the $N=20$ shell closure, and other more neutron-rich Na isotopes are well deformed with quadrupole deformation $\beta_2 > 0.35$. Therefore, the significant increase in density distribution along the symmetry axis from ^{31}Na to ^{33}Na in Fig. 5(a) can be understood from the deformation effects. From ^{33}Na to ^{41}Na , the neutron density distribution along the symmetry axis gradually becomes more diffuse with the increasing neutron number. In Fig. 5(b), similar gradual growth is seen in the neutron density distribution perpendicular to the symmetry axis from ^{31}Na to ^{37}Na . However, far away from the center, the density distributions of ^{39}Na and ^{41}Na are very diffuse, even though they are prolate deformed. This suggests oblate neutron halos in ^{39}Na and ^{41}Na , with the prolate-oblate shape decoupling for the core and halo.

Further analysis reveals that the $1/2^-$ and $3/2^-$ orbit-

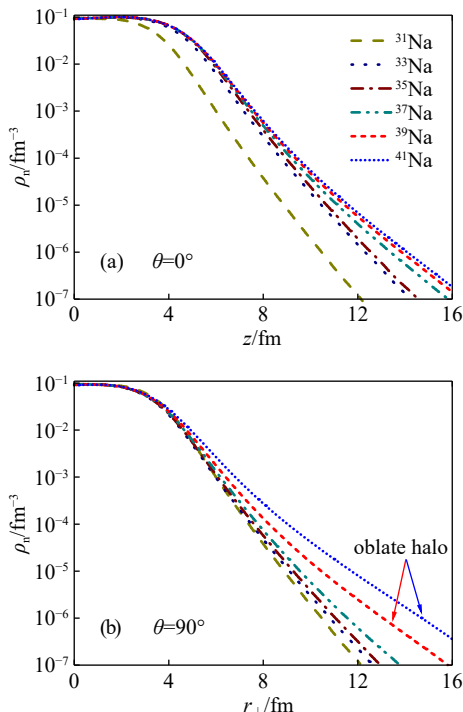


Fig. 5 Neutron density distributions (a) along ($\theta=0^\circ$) and (b) perpendicular to ($\theta=90^\circ$) the symmetry axis for neutron-rich odd-even sodium isotopes $^{31,33,\dots,41}\text{Na}$. In (b), $r_\perp = \sqrt{x^2 + y^2}$. Taken from Ref. [14]. (color online)

als embedded in continuum contribute predominantly to the halos in $^{39,41}\text{Na}$. These two orbitals have considerable p -wave components. According to the angular momentum coupling, both spherical harmonic functions $|Y_{10}(\theta, \varphi)|^2$ and $|Y_{1\pm 1}(\theta, \varphi)|^2$ contribute to the $1/2^-$ orbital, and the latter dominates. For the $3/2^-$ orbital, only $|Y_{1\pm 1}(\theta, \varphi)|^2$ contributes. The angular distribution is prolate for $|Y_{10}(\theta, \varphi)|^2 \propto \cos^2 \theta$ and is oblate for $|Y_{1\pm 1}(\theta, \varphi)|^2 \propto \sin^2 \theta$. The shape of the halo is thus oblate.

Therefore, based on the DRHBC calculations with density functional PC-PK1, the disappearance of the traditional magic number $N=28$ and the appearance of a deformed neutron halo in the new isotope ^{39}Na are predicted. For the results from other density functionals for Na isotopes, the discussion on the neutron drip-line location, and further exploration on the microscopic mechanism for the formation of halos, see Ref. [14].

2.3 The possible triaxial halo nucleus ^{42}Al

Non-axial deformation, namely, triaxial deformation, is one of the basic deformation degrees of freedom in atomic nuclei. The triaxiality is closely related to rich nuclear phenomena, e.g., the chiral rotation^[110], wobbling motion^[111], and fission^[112]. It is recently found that the information on nuclear deformation can be extracted from relativistic heavy-ion collision experiments^[113], and evidence for the triaxial structure in ^{129}Xe has been reported by analyzing the data from the CERN Large Hadron Collider^[114], which further stimulates the interest in triaxial nuclei.

It would be interesting to explore the possible existence of triaxial halo nuclei. In 2021, a calculation based on the Woods-Saxon potential suggests that the region of halo nuclei could be extended by triaxial deformation that allows the appearance of s - or p -wave components in some weakly bound orbitals^[115]. However, the triaxial deformation, the depth, and the width of the potential are adjustable parameters, and the crucial pairing and continuum effects are not included in such a phenomenological model. In contrast, the TRHBC theory takes into account the triaxial deformation, pairing correlations, and continuum effects in a microscopic and self-consistent way, making it capable of describing triaxial halo nuclei properly. The TRHBC theory predicts ^{42}Al as a triaxial halo nucleus by examining the neutron separation energies, rms radii, density distributions, and single-neutron orbitals around the Fermi energy for aluminum isotopes^[81].

Figure 6 exhibits the density distributions in xy , xz , and yz planes for the core and the halo of ^{42}Al , calculated from the TRHBC theory with PC-PK1. It can be found that the halo density is significantly more diffuse than the core density, especially in the yz plane. Quantitatively, the rms radius is 3.85 fm for the core and 5.26 fm for the halo. The

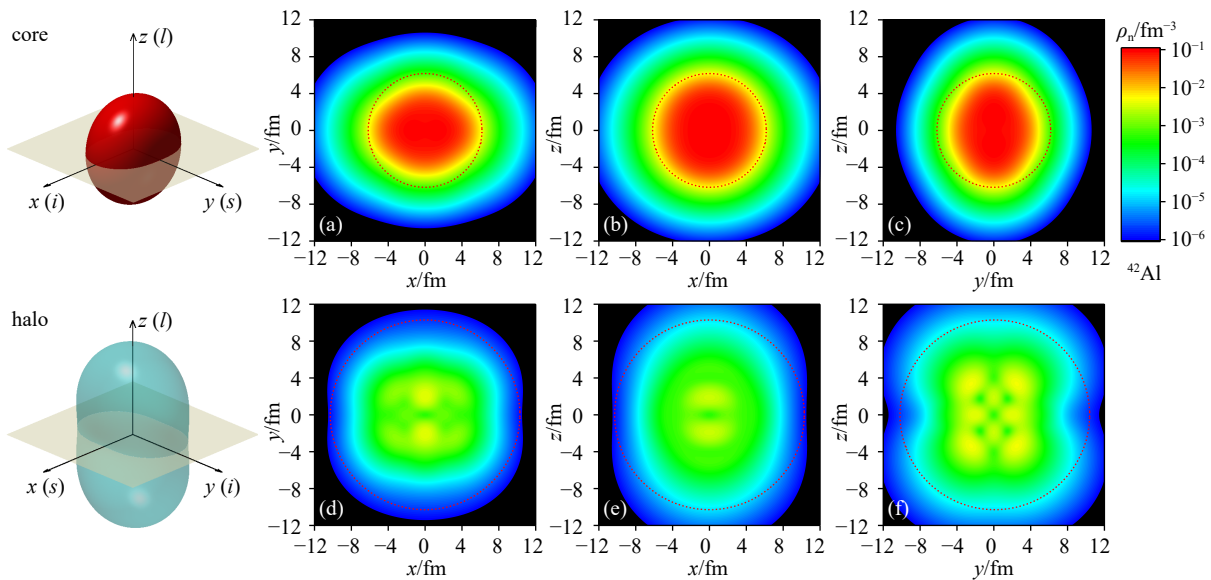


Fig. 6 Neutron density distributions in xy , xz , and yz planes for the core (a)~(c) and the halo (d)~(f) in the predicted triaxial halo nucleus ^{42}Al . In each plot, a circle in dotted line is drawn to guide the eye. With the rms radius and deformation parameters β and γ calculated from densities, the corresponding schematic shapes for the core and the halo are given in the left, in which s , i , and l respectively represent the short, intermediate, and long axes. Taken from Ref. [81] and slightly modified. (color online)

deformation parameters (β, γ) are $(0.38, 50^\circ)$ and $(0.79, -23^\circ)$ for the core and the halo, respectively. The negative γ value means that y is the intermediate axis while x is the short one. This is just the reverse of the case for the core. With the corresponding rms radius and deformation parameters, the schematic pictures for the core and the halo are also displayed in Fig. 6, where the long, intermediate, and short axes can be distinguished clearly. Therefore, ^{42}Al is a triaxial halo nucleus with a novel triaxial shape decoupling between the core and the halo. For detailed results and discussion on the triaxial halo characteristics of ^{42}Al , see Ref. [81].

3 Summary

The halo phenomena in exotic nuclei have long been an important frontier in nuclear physics research. The relativistic density functional theory has made great progress in the study of halo nuclei. Recently, a microscopic and self-consistent description of ^{37}Mg , including its small one-neutron separation energy, large rms radius, diffuse density distribution, and p -wave components for the halo neutron, has been obtained using the DRHBc theory^[54]. Based on the structure input purely from the DRHBc theory, the reaction cross section of ^{37}Mg on a carbon target and the momentum distribution of ^{36}Mg fragments after its breakup are reproduced very well by the Glauber model^[55]. Therefore, a unified description of the halo characteristics of ^{37}Mg from nuclear structure to reaction dynamics has been achieved.

The recently discovered isotope ^{39}Na has been investigated with the DRHBc theory^[14]. It is revealed that the

lowering of $2p$ orbitals in the spherical limit results in the disappearance of the $N=28$ magicity in ^{39}Na . The pairing correlations and the pf component mixing driven by deformation lead to the partial occupation of the weakly bound and continuum orbitals with certain p -wave components, giving rise to the formation of an oblate neutron halo around the prolate core in ^{39}Na .

To explore triaxial halo nuclei, the TRHBc theory has been developed, which self-consistently includes the triaxiality, pairing correlations, and continuum effects^[81]. The observed heaviest odd-odd aluminum isotope, ^{42}Al , is predicted as a triaxially deformed halo nucleus, in which a novel triaxial shape decoupling, *i.e.*, the exchange of the intermediate and short axes between the triaxial core and the triaxial halo, is found.

Acknowledgments Helpful discussions with members of the DRHBc Mass Table Collaboration, the collaboration with J. L. An, Y. Kim, J. Meng, M.-H. Mun, P. Papakonstantinou, X.-X. Sun, S. Q. Zhang, and S. S. Zhang, and the support from H. Yan are gratefully appreciated.

References:

- [1] TANIHATA I, HAMAGAKI H, HASHIMOTO O, et al. *Phys Rev Lett*, 1985, 55: 2676.
- [2] ZHUKOV M, DANILIN B, FEDOROV D, et al. *Phys Rep*, 1993, 231(4): 151.
- [3] HANSEN P G, JENSEN A S, JONSON B. *Annu Rev Nuc Part Sci*, 1995, 45(1): 591.
- [4] OTSUKA T, FUKUNISHI N, SAGAWA H. *Phys Rev Lett*, 1993, 70: 1385.
- [5] KUO T T S, KRMPOTIĆ F, TZENG Y. *Phys Rev Lett*, 1997, 78:

- [2708.]
- [6] HORIUCHI H, KANADA-EN' YO Y, ONO A. *Z Phys A*, 1994, 349(3): 279.
- [7] ITAGAKI N, AOYAMA S. *Phys Rev C*, 1999, 61: 024303.
- [8] RYBERG E, FORSSÉN C, HAMMER H W, et al. *Phys Rev C*, 2014, 89: 014325.
- [9] JI C, ELSTER C, PHILLIPS D R. *Phys Rev C*, 2014, 90: 044004.
- [10] TERASAKI J, HEENEN P H, FLOCARD H, et al. *Nucl Phys A*, 1996, 600(3): 371.
- [11] SCHUNCK N, EGIDO J L. *Phys Rev C*, 2008, 78: 064305.
- [12] MENG J, RING P. *Phys Rev Lett*, 1996, 77: 3963.
- [13] PÖSCHL W, VRETENAR D, LALAZISSIS G A, et al. *Phys Rev Lett*, 1997, 79: 3841.
- [14] ZHANG K Y, PAPAKONSTANTINOU P, MUN M H, et al. *Phys Rev C*, 2023, 107: L041303.
- [15] MENG J. International Review of Nuclear Physics: Volume 10 Relativistic Density Functional for Nuclear Structure[M/OL]. Singapore: World Scientific, 2016. DOI: 10.1142/9872.
- [16] RING P. *Phys Scr*, 2012, T150: 014035.
- [17] MENG J, ZHANG K Y. *Physics*, 2021, 50: 789. (in Chinese) (孟杰, 张开元. *物理*, 2021, 50: 789.)
- [18] KOEFPF W, RING P. *Z Phys A*, 1991, 339(1): 81.
- [19] REN Z X, ZHAO P W. *Phys Rev C*, 2020, 102: 021301(R).
- [20] SHARMA M M, LALAZISSIS G, KÖNIG J, et al. *Phys Rev Lett*, 1995, 74: 3744.
- [21] WALECKA J. *Ann Phys*, 1974, 83(2): 491.
- [22] GINOCCHIO J N. *Phys Rev Lett*, 1997, 78: 436.
- [23] MENG J, SUGAWARA-TANABE K, YAMAJI S, et al. *Phys Rev C*, 1998, 58: R628.
- [24] LIANG H, MENG J, ZHOU S G. *Phys Rep*, 2015, 570: 1.
- [25] ZHOU S G, MENG J, RING P. *Phys Rev Lett*, 2003, 91: 262501.
- [26] HE X T, ZHOU S G, MENG J, et al. *Eur Phys J A*, 2006, 28: 265.
- [27] KOEFPF W, RING P. *Nucl Phys A*, 1989, 493(1): 61.
- [28] KOEFPF W, RING P. *Nucl Phys A*, 1990, 511(2): 279.
- [29] RING P. *Prog Part Nucl Phys*, 1996, 37: 193.
- [30] VRETENAR D, AFANASJEV A V, LALAZISSIS G A, et al. *Phys Rep*, 2005, 409(3): 101.
- [31] MENG J, TOKI H, ZHOU S G, et al. *Prog Part Nucl Phys*, 2006, 57: 470.
- [32] MENG J, Guo J Y, Li J, et al. *Progress in Physics*, 2011, 31(04): 199. (in Chinese) (孟杰, 郭建友, 李剑, 等. *物理学进展*, 2011, 31(04): 199.)
- [33] NIKŠIĆ T, VRETENAR D, RING P. *Prog Part Nucl Phys*, 2011, 66(3): 519.
- [34] MENG J, PENG J, ZHANG S Q, et al. *Front Phys*, 2013, 8: 55.
- [35] MENG J, ZHOU S G. *J Phys G*, 2015, 42(9): 093101.
- [36] ZHOU S G. *Phys Scr*, 2016, 91(6): 063008.
- [37] SHEN S, LIANG H, LONG W H, et al. *Prog Part Nucl Phys*, 2019, 109: 103713.
- [38] MENG J, ZHAO P. *AAPPs Bull*, 2021, 31(1): 2.
- [39] MENG J. *Nucl Phys A*, 1998, 635: 3.
- [40] MENG J, RING P. *Phys Rev Lett*, 1998, 80: 460.
- [41] LÜ H F, MENG J, ZHANG S Q, et al. *Eur Phys J A*, 2003, 17: 19.
- [42] ZHOU S G, MENG J, RING P, et al. *Phys Rev C*, 2010, 82: 011301.
- [43] LI L, MENG J, RING P, et al. *Phys Rev C*, 2012, 85: 024312.
- [44] LI L, MENG J, RING P, et al. *Chin Phys Lett*, 2012, 29: 042101.
- [45] CHEN Y, LI L, LIANG H, et al. *Phys Rev C*, 2012, 85: 067301.
- [46] ZHOU S G, MENG J, RING P. *Phys Rev C*, 2003, 68: 034323.
- [47] COTTLE P D, KEMPER K W. *Physics*, 2012, 5: 49.
- [48] BAUMANN T, AMTHOR A M, BAZIN D, et al. *Nature*, 2007, 449(7165): 1022.
- [49] YANG Z H, KUBOTA Y, CORSI A, et al. *Phys Rev Lett*, 2021, 126: 082501.
- [50] SUN X X. *Phys Rev C*, 2021, 103: 054315.
- [51] SUN X X, ZHAO J, ZHOU S G. *Phys Lett B*, 2018, 785: 530.
- [52] SUN X X, ZHAO J, ZHOU S G. *Nucl Phys A*, 2020, 1003: 122011.
- [53] ZHONG S Y, ZHANG S S, SUN X X, et al. *Sci China Phys Mech Astron*, 2022, 65(6): 262011.
- [54] ZHANG K, YANG S, AN J, et al. *Phys Lett B*, 2023, 844: 138112.
- [55] AN J L, ZHANG K Y, LU Q, et al. *Phys Lett B*, 2024, 849: 138422.
- [56] ZHANG K, CHEOUN M K, CHOI Y B, et al. *Phys Rev C*, 2020, 102: 024314.
- [57] ZHANG K Y, PAN C, ZHANG S Q, et al. *Chin Sci Bull*, 2021, 66: 3561. (in Chinese) (张开元, 潘琮, 张双全, 孟杰. *科学通报*, 2021, 66: 3561.)
- [58] PAN C, CHEOUN M K, CHOI Y B, et al. *Phys Rev C*, 2022, 106: 014316.
- [59] GUO P, CAO X, CHEN K, et al. *arXiv*, 2024, 2402: 02935.
- [60] ZHANG K Y, WANG D Y, ZHANG S Q. *Phys Rev C*, 2019, 100: 034312.
- [61] IN E J, KIM Y, PAPAKONSTANTINOU P, et al. *J Korean Phys Soc*, 2020, 77(11): 966.
- [62] IN E J, PAPAKONSTANTINOU P, KIM Y, et al. *Int J Mod Phys E*, 2021, 30(02): 2150009.
- [63] ZHANG K, HE X, MENG J, et al. *Phys Rev C*, 2021, 104: L021301.
- [64] PAN C, ZHANG K Y, CHONG P S, et al. *Phys Rev C*, 2021, 104: 024331.
- [65] HE X T, WANG C, ZHANG K Y, et al. *Chin Phys C*, 2021, 45: 101001.
- [66] SUN W, ZHANG K Y, PAN C, et al. *Chin Phys C*, 2022, 46: 064103.
- [67] ZHANG X Y, NIU Z M, SUN W, et al. *Phys Rev C*, 2023, 108: 024310.
- [68] MUN M H, KIM S, CHEOUN M K, et al. *Phys Lett B*, 2023, 847: 138298.
- [69] GUO P, PAN C, ZHAO Y C, et al. *Phys Rev C*, 2023, 108: 014319.
- [70] SUN X X, ZHOU S G. *Sci Bull*, 2021, 66(20): 2072.
- [71] SUN X X, ZHOU S G. *Phys Rev C*, 2021, 104: 064319.
- [72] MISU T, NAZAREWICZ W, ABERG S. *Nucl Phys A*, 1997, 614(1): 44.
- [73] WATANABE S, MINOMO K, SHIMADA M, et al. *Phys Rev C*, 2014, 89: 044610.
- [74] LI X, HEENEN P H. *Phys Rev C*, 1996, 54: 1617.
- [75] PEI J, XU F, STEVENSON P. *Nucl Phys A*, 2006, 765(1): 29.
- [76] NAKADA H, TAKAYAMA K. *Phys Rev C*, 2018, 98: 011301.
- [77] KASUYA H, YOSHIDA K. *Prog Theor Exp Phys*, 2020, 2021(1):

- 013D01.
- [78] GENG J, LONG W H. *Phys Rev C*, 2022, 105: 034329.
- [79] GENG J, NIU Y F, LONG W H. *Chin Phys C*, 2023, 47(4): 044102.
- [80] CALCI A, NAVRÁTIL P, ROTH R, et al. *Phys Rev Lett*, 2016, 117: 242501.
- [81] ZHANG K Y, ZHANG S Q, MENG J. *Phys Rev C*, 2023, 108: L041301.
- [82] KUCHAREK H, RING P. *Z Phys A*, 1991, 339(1): 23.
- [83] XIANG Y, LUO Q, YANG S, et al. *Symmetry*, 2023, 15(7): 1420.
- [84] ZHANG K Y, PAN C, ZHANG S Q. *Phys Rev C*, 2022, 106: 024302.
- [85] PAN C, ZHANG K, ZHANG S. *Int J Mod Phys E*, 2019, 28(09): 1950082.
- [86] PEREZ-MARTIN S, ROBLEDO L M. *Phys Rev C*, 2008, 78: 014304.
- [87] KOBAYASHI N, NAKAMURA T, KONDO Y, et al. *Phys Rev Lett*, 2014, 112: 242501.
- [88] TAKECHI M, SUZUKI S, NISHIMURA D, et al. *Phys Rev C*, 2014, 90: 061305(R).
- [89] SAKURAI H, AOI N, GOTO A, et al. *Phys Rev C*, 1996, 54: R2802.
- [90] HAMAMOTO I. *Phys Rev C*, 2007, 76: 054319.
- [91] REN Z, ZHU Z, CAI Y, et al. *Phys Lett B*, 1996, 380(3): 241.
- [92] HORIUCHI W, INAKURA T, NAKATSUKASA T, et al. *Phys Rev C*, 2012, 86: 024614.
- [93] SHARMA M K, MEHTA M S, PATRA S K. *Int J Mod Phys E*, 2013, 22(01): 1350005.
- [94] XU X D, ZHANG S S, SIGNORACCI A J, et al. *Phys Rev C*, 2015, 92: 024324.
- [95] FANG Z, SHI M, GUO J Y, et al. *Phys Rev C*, 2017, 95: 024311.
- [96] SUN T T, QIAN L, CHEN C, et al. *Phys Rev C*, 2020, 101: 014321.
- [97] URATA Y, HAGINO K, SAGAWA H. *Phys Rev C*, 2017, 96: 064311.
- [98] CHOUDHARY V, HORIUCHI W, KIMURA M, et al. *Phys Rev C*, 2021, 104: 054313.
- [99] XIONG X Y, PEI J C, ZHANG Y N, et al. *Chin Phys C*, 2016, 40(2): 024101.
- [100] BÜRVENICH T, MADLAND D G, MARUHN J A, et al. *Phys Rev C*, 2002, 65: 044308.
- [101] ZHAO P W, LI Z P, YAO J M, et al. *Phys Rev C*, 2010, 82: 054319.
- [102] LALAZISSIS G A, KARATZIKOS S, FOSSION R, et al. *Phys Lett B*, 2009, 671(1): 36.
- [103] LONG W, MENG J, VAN GIAI N, et al. *Phys Rev C*, 2004, 69: 034319.
- [104] THOENNESSEN M. *The Discovery of Isotopes*[M/OL]. New York: Springer, 2016.
- [105] ZHANG Z Y, GAN Z G, YANG H B, et al. *Phys Rev Lett*, 2019, 122: 192503.
- [106] AHN D S, FUKUDA N, GEISSEL H, et al. *Phys Rev Lett*, 2019, 123: 212501.
- [107] AHN D S, AMANO J, BABA H, et al. *Phys Rev Lett*, 2022, 129: 212502.
- [108] BASTIN B, GRÉVY S, SOHLER D, et al. *Phys Rev Lett*, 2007, 99: 022503.
- [109] DOORNENBAL P, SCHEIT H, TAKEUCHI S, et al. *Phys Rev Lett*, 2013, 111: 212502.
- [110] FRAUENDORF S, MENG J. *Nucl Phys A*, 1997, 617: 131.
- [111] BOHR A, MOTTELSON B R. *Nuclear Structure: II*[M]. New York: Benjamin, 1975.
- [112] LU B N, ZHAO E G, ZHOU S G. *Phys Rev C*, 2012, 85: 011301.
- [113] GIACALONE G, JIA J, ZHANG C. *Phys Rev Lett*, 2021, 127: 242301.
- [114] BALLY B, BENDER M, GIACALONE G, et al. *Phys Rev Lett*, 2022, 128: 082301.
- [115] UZAWA K, HAGINO K, YOSHIDA K. *Phys Rev C*, 2021, 104: L011303.

相对论密度泛函理论研究晕核的近期进展

张开元¹, 潘琮^{2,†}, 陈思宇¹, 罗庆金¹, 吴柯岩¹, 向一峰¹

(1. 中国工程物理研究院核物理与化学研究所, 四川 绵阳 621900;
2. 安徽师范大学物理与电子信息学院, 安徽 芜湖 241000)

摘要: 自1985年实验发现晕核¹¹Li以来, 奇特原子核中的晕现象一直是核物理研究的重要前沿。相对论密度泛函理论在晕核研究中取得了很大成功, 如晕核¹¹Li的自洽描述和形变晕核的微观预言。介绍一些近期基于形变相对论连续谱 Hartree-Bogoliubov (DRHBc) 理论和三轴相对论连续谱 Hartree-Bogoliubov (TRHBc) 理论的研究进展。DRHBc 理论实现了对形变晕核³⁷Mg 的微观自洽描述, 再现了它的小中子分离能、大均方根半径、弥散密度分布以及晕中子的 p 波成分。DRHBc 理论还预言了最近发现的核素³⁹Na 中的形变中子晕以及 $N=28$ 闭壳的塌缩。新发展的 TRHBc 理论研究了铝同位素链, 预言最重的奇奇核⁴²Al 是三轴形变晕核, 并且它的核芯和晕存在三轴层次的新奇形状退耦。

关键词: 晕现象; 相对论密度泛函理论; ³⁷Mg; ³⁹Na; ⁴²Al

收稿日期: 2023-06-30; 修改日期: 2024-01-21

基金项目: 国家自然科学基金资助项目(12305125, U2230207, U2030209); 四川省自然科学基金资助项目(24NSFSC5910); 国家重点研发计划(2020YFA0406001, 2020YFA0406002)

†通信作者: 潘琮, E-mail: cpan@ahnu.edu.cn